

# Locations of multicritical points for spin glasses on regular lattices

Masayuki Ohzeki

Department of Physics, Tokyo Institute of Technology,  
Oh-okayama, Meguro-ku, Tokyo 152-8551, Japan

(Dated: October 30, 2018)

We present an analysis leading to precise locations of the multicritical points for spin glasses on regular lattices. The conventional technique for determination of the location of the multicritical point was previously derived using a hypothesis emerging from duality and the replica method. In the present study, we propose a systematic technique, by an improved technique, giving more precise locations of the multicritical points on the square, triangular, and hexagonal lattices by carefully examining relationship between two partition functions related with each other by the duality. We can find that the multicritical points of the  $\pm J$  Ising model are located at  $p_c = 0.890813$  on the square lattice, where  $p_c$  means the probability of  $J_{ij} = J(> 0)$ , at  $p_c = 0.835985$  on the triangular lattice, and at  $p_c = 0.932593$  on the hexagonal lattice. These results are in excellent agreement with recent numerical estimations.

## I. INTRODUCTION

The realistic world is affected by randomness. Unlike non-random systems, those with randomness sometimes show rich and complicated phenomena. One of the interesting issues for such random systems is spin glass.

Many studies mainly by the mean-field analysis have been successful to elucidate various concepts for understanding spin glasses [1, 2, 3]. One of the current issues in spin glasses is their nature in finite dimensions below the upper critical dimension. Unfortunately, for finite dimensions, we often rely on numerical simulations, because there are few ways to analytically study spin glasses in finite dimensions. We need long equilibration times for the numerical simulations for spin glasses and average over many realizations of random systems to make error bars small enough. It is thus difficult to give conclusive understanding on nature of spin glasses in finite dimensions.

To establish reliable analytical theories of spin glasses has been one of the most challenging problems for years. A part of successful analyses to elucidate properties on spin glasses is by the use of the gauge symmetry. By use of the gauge symmetry, one can obtain the exact value of the internal energy, evaluate the upper bound for the specific heat, and obtain some correlation inequalities in a subspace known as the Nishimori line [4, 5]. This gauge symmetry also enables us to rewrite the free energy along the Nishimori line as the entropy for the distribution of frustration [6]. Many aspects on spin glasses are essentially related with frustration. Therefore we expect the possibility that a basis of establishment of a systematic approach to spin glasses would be in the gauge symmetry.

A recent related development with the gauge symmetry is the *conjecture* to predict the location of the multicritical point, which is the special point lying on the intersection between phase boundaries and the Nishimori line as in Fig. 1 [7, 8, 9, 10, 11, 12]. The predictions by the conjecture have shown agreement with numerical estimations roughly with precision to the third digit. The conjecture has opened a way of a general scheme for determi-

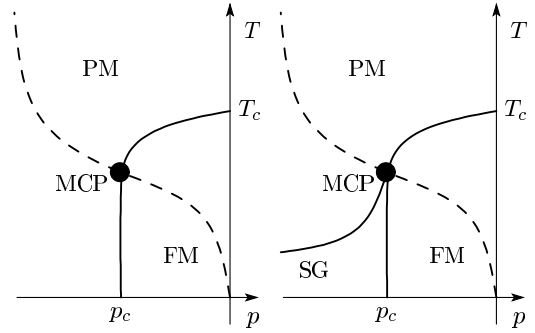


FIG. 1: Phase diagram of the  $\pm J$  Ising model on two-dimensional lattice (left panel) and on higher dimensions (right panel). The vertical axis expresses the temperature  $T$ , and the horizontal line denotes the concentration  $p$  of the antiferromagnetic interactions. The multicritical point is described by the black point (MCP). The Nishimori line is described by the dashed line. For higher dimensions, not only the ferromagnetic (FM) and paramagnetic phases (PM) but also the spin glass phase (SG) exists.

nation of the location of the multicritical points for spin glasses on any self-dual lattices and mutually dual pairs of lattices. Nevertheless it has been found that the conjecture on several mutually dual pairs of hierarchical lattices does not always give predictions in agreement with estimations by the renormalization group analysis [13]. Such discrepancies are not negligible, because the renormalization group analysis on hierarchical lattices gives exact solutions. To construct a more reliable technique, we have improved the technique leading to the location of the multicritical point by combining the concepts of the renormalization group analysis with the duality [14]. The improvement for hierarchical lattices has greatly succeeded as seen in the literature, because the discrepancies between the predictions by the improved technique and the exact estimations by the renormalization group analysis actually decrease. Reconsidering the improved

technique on the hierarchical lattices, in this paper, we apply the improved technique to the regular lattices such as the square, triangular, and hexagonal lattices.

The present paper is organized as follows. In Sec. II, we introduce the conventional conjecture and take a look at several published predictions. In addition, the problem on the conjecture is pointed out here. The improved technique on the regular lattices is proposed after review of the case on the hierarchical lattices in Sec. III, and formulated in Sec. IV. The improved version shows a very close relationship with the entropy of the distribution of frustration as shown in this section. In Sec. V, we carry out the explicit calculations by the improved technique for the regular lattices. Moreover we have to carefully evaluate the performance of the improved technique, comparing their predictions with the existing results. We examine the correspondence with the Domany's exact result [15, 16] of the slope of the critical point on the phase diagram. The conclusion is in the last section of the present paper, Sec. VII.

## II. CONVENTIONAL CONJECTURE

### A. Duality

It will be useful to review the analysis by the duality, for the conjecture is established by combination of the duality and the replica method [7, 8]. The duality is one of the tools to identify the transition points for various types of classical spin systems such as the Ising model, and the Potts model by use of a symmetry embedded in the partition function [17]. We take the non-random Ising model on the square lattice as an example. The partition function is given as

$$Z(\beta) = \sum_{\{S_i\}} \prod_{\langle ij \rangle} \exp(\beta J S_i S_j) \quad (1)$$

Where  $S_i$  is the Ising spin taking  $\pm 1$  and the product with the subscript  $\langle ij \rangle$  is over the nearest neighboring sites. We can regard this partition function as the multi-variable function of components of the edge Boltzmann factor. In this case, the edge Boltzmann factor is  $\exp(\beta J S_i S_j)$ . We consider that the dependence on  $\beta$  emerges through this edge Boltzmann factors. We set two components as  $x_0(\beta) = e^{\beta J}$  and  $x_1(\beta) = e^{-\beta J}$  for convenience. The component  $x_0(\beta)$  is often called the principal Boltzmann factor, which is defined by the edge Boltzmann factor for the state with all edge spins parallel. The principal Boltzmann factor is an important component throughout this paper. The duality is carried out by the Fourier transformation for this edge Boltzmann factor defined on each bond of the lattice [18]. The two-component Fourier transformation gives the dual edge

Boltzmann factors as,

$$x_0(\beta)^* = \frac{1}{\sqrt{2}} (e^{\beta J} + e^{-\beta J}) \quad (2)$$

$$x_1(\beta)^* = \frac{1}{\sqrt{2}} (e^{\beta J} - e^{-\beta J}). \quad (3)$$

As a result, we establish the relation between the partition functions with different components as,

$$Z(x_0, x_1) = Z(x_0^*, x_1^*). \quad (4)$$

We here extract two principal Boltzmann factors  $x_0$  and  $x_0^*$  to measure the energy from the state with edge spins on each bond being parallel as,

$$x_0^{N_B}(\beta) z(u_1) = x_0^{*N_B}(\beta) z(u_1^*). \quad (5)$$

where  $N_B$  stands for the number of bonds, and  $u_1$  and  $u_1^*$  are called the relative Boltzmann factors defined as  $u_1(\beta) = x_1(\beta)/x_0(\beta)$  and  $u_1^*(\beta) = x_1^*(\beta)/x_0^*(\beta)$ . Each partition function is now reduced to a single-variable function of  $u_1$  and  $u_1^*$ , whose explicit forms are,

$$u_1(\beta) = e^{-2\beta J} \quad (6)$$

$$u_1^*(\beta) = \tanh \beta J. \quad (7)$$

Being very well known, the duality relation can be given as  $e^{-2\beta^* J} = \tanh \beta J$  to think of the dual partition function as one of another Ising model with the edge Boltzmann factor  $e^{\beta^* J \sigma_i \sigma_j}$ . We can identify the critical point as a fixed point of the duality as  $e^{-2\beta_c} = \tanh \beta_c J$ , under the assumption of a unique transition. On this critical point, an appealing equation is satisfied  $x_0 = x_0^*$ .

### B. Duality for the quenched system

We consider the case of the random-bond Ising model and review the conventional conjecture [7, 8]. The Hamiltonian is defined by

$$H = - \sum_{\langle ij \rangle} J_{ij} S_i S_j, \quad (8)$$

where  $J_{ij}$  denotes the quenched random coupling and the summation is over the nearest neighboring sites. Though various types of distribution for  $J_{ij}$  can be considered, we here restrict ourselves to the  $\pm J$  Ising model for convenience. The distribution function for the  $\pm J$  Ising model is given by

$$P(J_{ij}) = p\delta(J_{ij} - J) + (1-p)\delta(J_{ij} + J) = \frac{e^{\beta_p J_{ij}}}{2 \cosh \beta_p J}, \quad (9)$$

where  $\beta_p$  is defined by  $e^{-2\beta_p J} = (1-p)/p$ . The Nishimori line is given by the condition  $\beta = \beta_p$  and is described by the dashed line in each phase diagram of Fig. 1.

We apply the replica method to the  $\pm J$  Ising model on the Nishimori line as,

$$Z(\beta_p, \beta_p) = \left[ \sum_{\{S_i\}} \prod_{\alpha=1}^n \exp(\beta_p J_{ij} S_i^\alpha S_j^\alpha) \right]_{\text{av}} \quad (10)$$

where  $n$  stands for the replica number and the angular brackets denote the configurational average. We apply the duality argument as reviewed above to this  $n$ -replicated  $\pm J$  Ising model. The duality gives the relationship of the partition functions with different components of the edge Boltzmann factor,

$$\begin{aligned} Z_n(x_0, x_1, \dots, x_n) \\ = Z_n(x_0^*, x_1^*, \dots, x_n^*), \end{aligned} \quad (11)$$

where the subscript of  $x$  and  $x^*$  denotes the number of antiparallel-spin pairs among the  $n$  replicas. Two principal Boltzmann factors  $x_0$  and  $x_0^*$  are given as [7, 8],

$$x_0(\beta) = [e^{n\beta J_{ij}}]_{\text{av}}, \quad (12)$$

$$x_0^*(\beta) = [2^{\frac{n}{2}} \cosh^n \beta J_{ij}]_{\text{av}}. \quad (13)$$

We extract these principal Boltzmann factors similarly to the case of the non-random bond Ising model,

$$\begin{aligned} x_0(\beta)^{N_B} z_n(u_1, u_2, \dots, u_n) \\ = x_0^*(\beta)^{N_B} z_n(u_1^*, u_2^*, \dots, u_n^*). \end{aligned} \quad (14)$$

We remark that the partition function for the  $n$ -replicated  $\pm J$  Ising model is a multi-variable function of the edge Boltzmann factors yet differently from the case of the non-random bond Ising model.

### C. Conjecture

We describe schematically the relationship two reduced partition functions  $z_n$  as the curves of the relative Boltzmann factors  $(u_1(\beta), u_2(\beta), \dots, u_n(\beta))$  (the thin curve going through the multicritical point  $p_c$ ) and  $(u_1^*(\beta), u_2^*(\beta), \dots, u_n^*(\beta))$  (the dashed line) as in Fig. 2. We now consider the relationship between these curves by the projections on the two-dimensional plane  $(u_1, u_2)$  for convenience. As the temperature changes from 0 to  $\infty$ , the representative point  $(u_1(\beta), u_2(\beta), \dots, u_n(\beta))$  moves toward the point P (the high-temperature limit) along the thin line in Fig. 2. Then the corresponding dual point  $(u_1^*(\beta), u_2^*(\beta), \dots, u_n^*(\beta))$  moves along the dashed line in the opposite direction from P to F (the low-temperature limit). These features have been shown rigorously and imply the existence of the duality relation for the temperature [12]. If two curves describing change of  $(u_1(\beta), u_2(\beta), \dots, u_n(\beta))$  and  $(u_1^*(\beta), u_2^*(\beta), \dots, u_n^*(\beta))$  become completely coincident with each other, we can obtain a relation  $u_r(\beta^*) = u_r(\beta)$ . Solving this relation, we obtain the duality relation for the temperature  $\beta^*(\beta)$ .

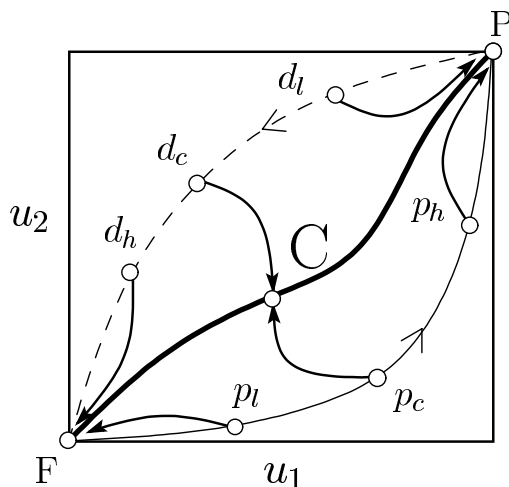


FIG. 2: Schematic picture of the duality and the renormalization flow for the replicated  $\pm J$  Ising model.

The well-known duality relation  $e^{-2\beta^* J} = \tanh \beta J$  for the non-random Ising model can be indeed derived from the relation  $u_r(\beta^*) = u_r^*(\beta)$ . Unfortunately the thin curve  $(u_1(\beta), u_2(\beta), \dots, u_n(\beta))$  does not coincide with the dashed curve  $(u_1^*(\beta), u_2^*(\beta), \dots, u_n^*(\beta))$  for the replicated  $\pm J$  Ising model on the Nishimori line as shown schematically in Fig. 2. In the case for the replicated  $\pm J$  Ising model, we can neither find a duality relation for the temperature explicitly, nor identify the multicritical point as the fixed point of duality.

We thus have provided a hypothesis on determination of the multicritical point [7, 8]. We assume that the equation  $x_0(\beta) = x_0^*(\beta)$  is also satisfied at the multicritical point, similarly to the non-random bond Ising model at the critical point, for any  $n$ -replicated systems including the quenched system ( $n \rightarrow 0$ ) [7, 8, 9, 10, 11, 12]. Validity of this hypothesis can be rigorously shown for  $n = 1$  and 2, and for  $n = \infty$ , and has been numerically confirmed for the  $n = 3$  case of the replicated  $\pm J$  Ising model on the square lattice within error bars of the numerical simulation [8]. Relying on these facts, we assume that we can predict the location of the multicritical point for the  $\pm J$  Ising model on the square lattice by the single equation  $x_0(\beta) = x_0^*(\beta)$ . The quenched limit  $n \rightarrow 0$  for this equation yields [7, 8],

$$-p \log p - (1-p) \log(1-p) = \frac{1}{2} \log 2. \quad (15)$$

The solution to this equation is  $p_c = 0.889972$ . We can also predict the location of the multicritical point for other types of randomness. For instance, that of the Gaussian Ising model with the mean  $J_0$  and the variance  $J = 1$  is given as  $J_0 = 1.021770$  [7, 8].

The conjecture can be extended to mutually dual pair lattices by considering the product of two partition functions with different couplings indicating two multicrit-

type	conjecture	numerical result
SQ $\pm J$	$p_c = 0.889972$ [7, 8]	0.8905(5) [19]
		0.8906(2)[20, 21]
		0.8907(2)[22]
		0.8894(9)[23]
		0.8900(5)[24]
		0.89081(7)[25]
SQ Gaussian	$J_0 = 1.021770$ [7, 8]	1.02098(4)[21]
TR $\pm J$	$p_c = 0.835806$ [11]	0.8355(5)[24]
TR Gaussian	$J_0 = 0.798174$	–
HEX $\pm J$	$p_c = 0.932704$ [11]	0.9325(5)[24]
HEX Gaussian	$J_0 = 1.270615$	–

TABLE I: Comparisons among the results derived by the conventional conjecture and the existing numerical results. SQ denotes the square lattice, TR means the triangular lattice, and HEX means the hexagonal lattice.

ical points [10], and we can obtain a relation between these multicritical points. We can predict the location of the multicritical point on the triangular lattice, though it is the mutually dual pair with the hexagonal lattice, by simultaneous use of the star-triangle transformation [11]. Through these extensions of the conjecture, we have predicted locations of the multicritical points for various cases, which show good consistencies with other estimations with high precision in spite of the simplicity, as seen in Table I.

On the other hand, the conjecture has given approximate locations of the multicritical points on several hierarchical lattices with the largest discrepancy of 3% [13]. We have inferred that the issue yielding such discrepancies comes from the following fact. Unlike the non-random Ising model, two lines do not coincide as shown in Fig. 2. Nevertheless we have assumed that the equation  $x_0 = x_0^*$  is satisfied. As shown in next section, the technique used in the conjecture has indeed been improved by reconsideration of these problems.

### III. IMPROVED TECHNIQUE

#### A. Renormalization Flow

We here introduce a new point of view from renormalization group, which has helped us to improve the technique on the location of the multicritical point on the hierarchical lattices [14]. In the present study, we apply this idea to the regular lattices. Two features through the renormalization group analysis on the hierarchical lattices are found. (i) The partition function does not change its functional form by renormalization; only the values of coupling constants change because of specialty of hierarchical lattices. (ii) The renormalization flow starting from a critical point is attracted toward an unstable fixed point. The feature (i) permits us to ex-

press the renormalization flow following the arrows emanating from  $p_c$  and  $d_c$  to C,  $p_h$  and  $d_l$  to P, and  $p_l$  and  $d_h$  to F as in Fig. 2. By the feature (ii), there is the renormalization flow from the multicritical point  $p_c$  and corresponding dual point  $d_c$ , which reaches the unstable fixed point C,  $(u_1^{(\infty)}, u_2^{(\infty)}, \dots, u_n^{(\infty)})$ , where the superscripts mean the number of steps of renormalization. Considering the two properties of the renormalization flow, we can find that the duality relates two trajectories from  $p_c$  and from  $d_c$ , tracing the renormalization flows at each renormalization. In other words, after a sufficient number of renormalization steps, the thin curve representing the original system and the dashed curve for the dual system both approach a common renormalized system represented by the bold line in Fig. 2, which goes through the unstable fixed point C. On this bold line, the partition function can behave as a single-variable function and we can identify the unstable fixed point by a single equation  $x_0(K) = x_0^*(K)$  similarly to the case of the non-random Ising model. This fact enables us to assume to predict the exact location of the multicritical point by the following equation,

$$x_0^{(\infty)}(\beta) = x_0^{*(\infty)}(\beta). \quad (16)$$

However it is difficult in general to evaluate this equation. We therefore have proposed a first-approximation equation  $x_0^{(1)} = x_0^{*(1)}$  as the improved technique. This equation has indeed led to more precise results than the relation  $x_0(\beta) = x_0^*(\beta)$  does [14].

#### B. Partial Summation

We step in the stage of establishment of the improved technique on regular lattices. Unfortunately, if we apply the above renormalization group analysis to the regular lattices, the feature (i) may be incorrect, because other types of many-body interactions are generated after each renormalization. In addition, the renormalization group analysis for the regular lattice is usually regarded as an approximate tool, because many-body interactions appear after the renormalization which prevents us from iterating the renormalization. If we attempt to construct the recursion relation of the renormalization for regular lattices, we introduce some approximations. However we recall that the improved technique on the hierarchical lattice has been successful within satisfactory precision even by a one-step renormalization [14]. We then sum over internal sites only in a unit cell of each hierarchical lattice. For example, we show such a calculation explicitly for the non-random Ising model on a self-dual hierarchical lattice in Fig. 3.

$$Ae^{\beta^{(2)}JS_iS_j} = \sum_{S_1, S_2} e^{\beta^{(1)}J(S_iS_1+S_iS_2+S_1S_2+S_1S_j+S_2S_j)}, \quad (17)$$

where  $A$  is the extra coefficient yielded by the renormalization. The left-hand side corresponds to the principal

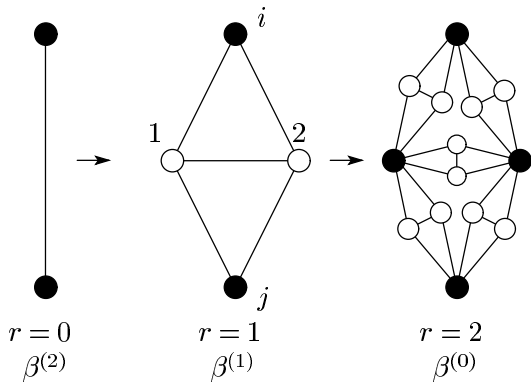


FIG. 3: A self-dual hierarchical lattice. The number  $r$  represents the step of the construction of the hierarchical lattice. The renormalized inverse temperature is expressed by  $\beta^{(l)}$ , where  $l$  is the step of the renormalization.

Boltzmann factor after one-step renormalization when  $S_i S_j = 1$ . We can regard this renormalized principal Boltzmann factor as the partition function defined on the unit cell of the hierarchical lattice in Fig. 3 under the constraint that the spins at both ends are parallel. In other words, the principal Boltzmann factor for the improved technique is in general given as

$$Z(\beta) = \overline{\sum_{\{S_i\}} \prod_{\langle ij \rangle}^{\text{unit}} e^{\beta^{(0)} J S_i S_j}} \quad (18)$$

where the overline means the summation over internal spins  $S_1$  and  $S_2$  on the unit cell of the hierarchical lattice with the spins on the edge up  $S_i$  and  $S_j = 1$ . The product runs over the nearest neighboring pairs on the unit of the hierarchical lattice. For the case for the random-bond Ising model, after application of the replica method, we also obtain the similar principal Boltzmann factor to the above example, by performing the partial summation over the unit of the hierarchical lattice. Instead of iterating summation as the renormalization, we sum partially over sites on the regular lattice. After we partially trace out the degrees of freedom in some area of the regular lattice, we regard the partition function on this area as the principal Boltzmann factor as the above example. We are able to construct the improved technique for the regular lattice without neglecting many-body interactions emerging after the summation. We call the limited-summation area of the regular lattice the cluster in this paper, and we define the partition function on the cluster as the principal Boltzmann factor for the improved technique on the regular lattice. When we take the summation over the internal sites, we impose the fixed boundary condition on all the spins on the boundary of the cluster as we have done for edge Boltzmann factor in the conventional conjecture.

We remark the possibility of the performance of the improved technique. Even if we partially sum over degrees

of freedom on the regular lattice as considered above, it is necessary to use an infinite-dimensional space to simultaneously express changes and generations of various types of many-body interactions. In this infinite dimensional space, we assume that there are two renormalization flows going uniformly toward the unstable fixed point, similarly to the case on hierarchical lattices. It is not able to examine such behaviors of the renormalization flows in the infinite-dimensional space and we cannot verify this assumption. Equation  $x_0 = x_0^*$  on the cluster may hence be a worse approximation than the conventional conjecture  $x_0^{(0)} = x_0^{*(0)}$  by consideration on a single bond. We have to carefully evaluate the performance of the improved technique for the regular lattices. At least, the obtained results as seen later can, however, give an answer for the location of the multicritical point for the  $\pm J$  Ising model on the square lattice with the precision to the fourth digit.

In addition, we will consider several types of the improvements for the regular lattice. On the hierarchical lattices, sufficient renormalization enables us to obtain the exact solution. Therefore we can expect that the improved technique for the hierarchical lattices gives more precise answers if we use the principal Boltzmann factor after more renormalization steps. On the regular lattices, it is considered that the performance of the improved technique depends on the area of the cluster. The number of degrees of freedom partially summed over on the regular lattice would correspond the step of the renormalization on the hierarchical lattice. We propose a few types of the clusters including several bonds below, considering this assumption.

## IV. FORMULATION

### A. Square Lattice

The starting point for the establishment of the improved technique is the exact duality relation (11) for the  $n$ -replicated partition function. As shown in Fig. 4, we consider to sum over a part of the spins on the square lattice. Then the exact duality relation (11) is reduced to

$$Z_n^{(s)}(x_0^{(s)}, x_1^{(s)}, \dots, x_n^{(s)}) = Z_n^{(s)}(x_0^{*(s)}, x_1^{*(s)}, \dots, x_n^{*(s)}). \quad (19)$$

Here  $Z_n^{(s)}$  represents the reduced partition function by the summation of a part of spins on the square lattice. The superscript  $s$  distinguishes the type of the approximations, for we consider different types of the summation below. The quantity  $x_k^{(s)}$  is the edge Boltzmann factor including many-body interactions generated after the summation. We take a cluster of the square lattice as in Fig. 4 and define the principal Boltzmann factors

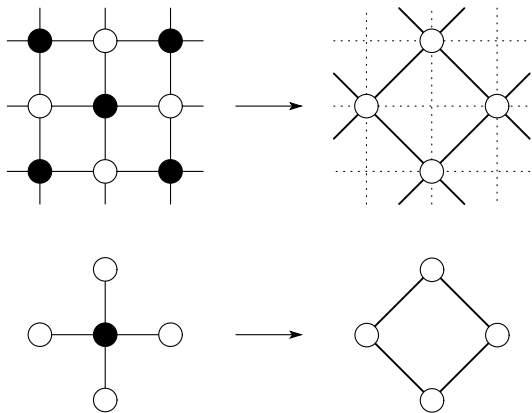


FIG. 4: Example of the partial summation for the square lattice and the cluster. The top figures describe one of the types of the summation for the square lattice. The bottom figures express the cluster for the principal Boltzmann factor.

after the summation,

$$x_0^{(s)} = \left[ \left\{ \overline{\sum_{\{S_i\}}^{\text{part}} \prod_{\langle ij \rangle} e^{\beta J_{ij} S_i S_j}} \right\}^n \right]_{\text{av}} \quad (20)$$

$$x_0^{*(s)} = \left[ \left\{ \overline{\sum_{\{S_i\}}^{\text{part}} \frac{1}{\sqrt{2}} (e^{\beta J_{ij}} + e^{-\beta J_{ij}} S_i S_j)} \right\}^n \right]_{\text{av}}, \quad (21)$$

where the overline means the summation over internal spins in the cluster of the square lattice as the filled circle in Fig. 4 with the other spins fixed to up directions  $\{S_i = 1\}$  represented by the white circles in Fig. 4. The word “part” represents that the product runs over the bonds of the cluster under consideration. These principal Boltzmann factors can be regarded as partition functions after the configurational average and application of the replica method defined on the cluster under the fixed boundary condition as shown in Fig. 4.

We assume that a single equation gives the critical points for any number of  $n$ , similarly to the conventional conjecture,

$$x_0^{(s)} = x_0^{*(s)}. \quad (22)$$

By the extrapolation of the quenched limit  $n \rightarrow 0$  of this equation, we establish the improved technique for the square lattice as follows,

$$\left[ \log Z^{*(s)}(\beta, \{J_{ij}\}) \right]_{\text{av}} - \left[ \log Z^{(s)}(\beta, \{J_{ij}\}) \right]_{\text{av}} = 0. \quad (23)$$

We need the configurational average for  $J_{ij}$  of the logarithmic terms by two partition functions  $Z^{(s)}$  and  $Z^{*(s)}$

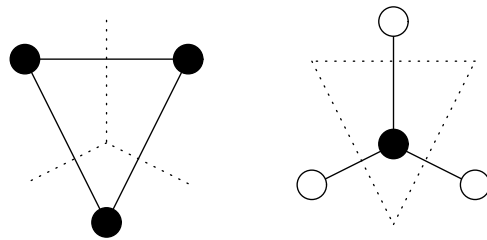


FIG. 5: Duality for the triangular lattice. After the duality transformation, the partition function on the triangular lattice is transformed into another partition function on the hexagonal lattice.

defined on the cluster,

$$Z^{(s)}(\beta, \{J_{ij}\}) = \overline{\sum_{\{S_i\}}^{\text{part}} \prod_{\langle ij \rangle} e^{\beta J_{ij} S_i S_j}} \quad (24)$$

$$Z^{*(s)}(\beta, \{J_{ij}\}) = \overline{\sum_{\{S_i\}}^{\text{part}} \prod_{\langle ij \rangle} \frac{1}{\sqrt{2}} (e^{\beta J_{ij}} + e^{-\beta J_{ij}} S_i S_j)}, \quad (25)$$

where the asterisk means that the edge Boltzmann factor is given in a different form obtained after the duality for the  $\pm J$  Ising model. We can estimate the location of the multicritical point by the above relation (23) as detailed below.

## B. Triangular Lattice

Similarly to the case on the square lattice, we can derive the improved technique for the triangular lattice. We give first several remarks on the duality with the star-triangle transformation. For the triangular lattice, it is convenient to use the face Boltzmann factor instead of the edge Boltzmann factor. The original face Boltzmann factor has three edge Boltzmann factors defined on the bonds of the elementary triangle. On the other hand, the dual face Boltzmann factor has three dual edge Boltzmann factors defined on the bonds on the star shape as in Fig. 5 [11, 26]. In the dual face Boltzmann factor, the summation over the spin at the center of the star is included, which corresponds to the star-triangle transformation. Similarly to the case of the square lattice, we start from the exact duality relation for the replicated random-bond Ising model on the triangular lattice,

$$Z_{\text{TR},n}(A_0, A_1, \dots) = Z_{\text{TR},n}^{(s)}(A_0^*, A_1^*, \dots), \quad (26)$$

where  $A$  and  $A^*$  are the original and dual face Boltzmann factors. We consider the summation over a part of the spins on the triangular lattice as in Fig. 6, and then this

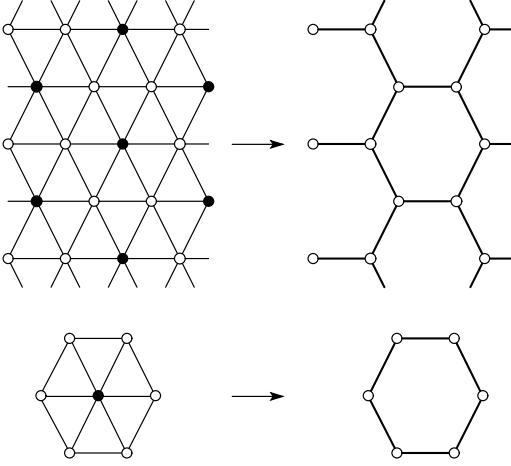


FIG. 6: Example of the summation for the triangular lattice and the cluster. The top figures express one of the types of the summation for the triangular lattice. The bottom figures express the cluster for the evaluation of the principal Boltzmann factor.

equation is reduced to,

$$Z_{\text{TR},n}^{(s)}(A_0^{(s)}, A_1^{(s)}, \dots) = Z_{\text{TR},n}^{(s)}(A_0^{*(s)}, A_1^{*(s)}, \dots), \quad (27)$$

where  $Z_{\text{TR},n}^{(s)}$  represents the reduced partition function by the summation over a part of spins on the triangular lattice. The quantity  $A_k^{(s)}$  is the face Boltzmann factor after the summation. We define the principal Boltzmann factor after the summation over a part of the triangular lattices as,

$$A_0^{(s)} = \left[ \left\{ \overline{\sum_{\{S_i\}}^{\text{part}} \prod_{\Delta} e^{\beta J_{12} S_1 S_2 + \beta J_{23} S_2 S_3 + \beta J_{31} S_3 S_1}} \right\}^n \right]_{\text{av}}, \quad (28)$$

$$A_0^{*(s)} = \left[ 2^{-\frac{n}{2} N_s^{(s)}} \times \left\{ \overline{\sum_{\{S_i\}} \sum_{\{S_0\}} \prod_{\Delta} \frac{1}{\sqrt{2}} (e^{\beta J_{10}} + e^{-\beta J_{10}} S_1 S_0)} \right. \right. \\ \times \frac{1}{\sqrt{2}} (e^{\beta J_{20}} + e^{-\beta J_{20}} S_2 S_0) \\ \left. \left. \times \frac{1}{\sqrt{2}} (e^{\beta J_{30}} + e^{-\beta J_{30}} S_3 S_0) \right\}^n \right]_{\text{av}}, \quad (29)$$

where  $N_s^{(s)}$  is equal to the number of the up-pointing triangles included in the cluster. The overline means the summation over internal spins included in the cluster of the triangular lattice as the filled circles in Fig. 6 with the other spins (the white circles) up  $\{S_i = 1\}$ . The word ‘‘part’’ represents summation over the up-pointing

triangles in the cluster as in Fig. 6. The summation over  $S_0$  means the star-triangle transformation. We can establish the improved technique for the triangular lattice by an equation of these principal Boltzmann factors after the summation  $A_0^{(s)} = A_0^{*(s)}$  and by the extrapolation to the quenched limit of  $n \rightarrow 0$ ,

$$\left[ \log Z_{\text{TR}}^{*(s)}(\beta, \{J_{ij}\}) \right]_{\text{av}} - \left[ \log Z_{\text{TR}}^{(s)}(\beta, \{J_{ij}\}) \right]_{\text{av}} = 0, \quad (30)$$

where the partition functions  $Z_{\text{TR}}^{*(s)}$  and  $Z_{\text{TR}}^{(s)}$  on the cluster of the triangular lattice are defined as,

$$Z_{\text{TR}}^{(s)}(\beta, \{J_{ij}\}) = \left[ \overline{\sum_{\{S_i\}}^{\text{part}} \prod_{\Delta} e^{\beta J_{12} S_1 S_2 + \beta J_{23} S_2 S_3 + \beta J_{31} S_3 S_1}} \right]_{\text{av}} \quad (31)$$

$$Z_{\text{TR}}^{*(s)}(\beta, \{J_{ij}\}) = \left[ 2^{-\frac{1}{2} N_s^{(s)}} \overline{\sum_{\{S_i\}} \sum_{\{S_0\}}^{\text{part}} \prod_{\Delta} \frac{1}{\sqrt{2}} (e^{\beta J_{10}} + e^{-\beta J_{10}} S_1 S_0)} \right. \\ \times \frac{1}{\sqrt{2}} (e^{\beta J_{20}} + e^{-\beta J_{20}} S_2 S_0) \\ \left. \times \frac{1}{\sqrt{2}} (e^{\beta J_{30}} + e^{-\beta J_{30}} S_3 S_0) \right]_{\text{av}}. \quad (32)$$

### C. Frustration Entropy and Multicritical Point

Before going into the detailed calculations for determination of the locations of the multicritical points, we consider the physical meaning of the improved technique from a different point of view. We show the relationship between the improved technique and the gauge symmetry, by taking the case of the square lattice as an example. The observation below implies the existence of deeply physical meaning behind the multicritical point. We will discuss the structure of the phase diagram by use of the connection between the improved technique and the gauge symmetry as shown below in the following section.

The second term  $Z^{(s)}$  on the left-hand side of Eq. (23) can be regarded as the free energy for the random-bond Ising model defined on the cluster if divided by  $\beta$ . The free energy for the gauge invariant model can be reduced to another form by the gauge transformation defined as [4, 5],

$$J_{ij} \rightarrow J_{ij} \sigma_i \sigma_j \quad (33)$$

$$S_i \rightarrow S_i \sigma_i, \quad (34)$$

where  $\sigma_i$  takes either  $-1$  or  $+1$ . We can obtain a useful expression of  $\log Z^{(s)}$  for the case of the  $\pm J$  Ising model

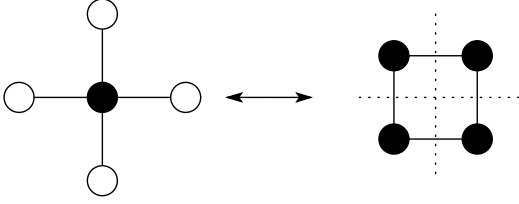


FIG. 7: Dual lattice for the cluster in Fig. 4. The black colored sites are free spins as the targets of the summation and the white ones are fixed in the up-pointing directions.

for instance [6],

$$\begin{aligned} & \left[ \log Z^{(s)}(\beta, \{J_{ij}\}) \right]_{\text{av}} \\ &= \frac{1}{2^{N_s^{(s)}} (2 \cosh \beta_p J)^{N_B^{(s)}}} \\ & \times \sum_{\{J_{ij}\}} Z^{(s)}(\beta_p, \{J_{ij}\}) \log Z^{(s)}(\beta, \{J_{ij}\}), \end{aligned} \quad (35)$$

where  $N_B^{(s)}$  is the number of bonds included in the cluster. In this expression, we obtain the entropy of the distribution of frustration on the cluster by setting  $\beta = \beta_p$ .

On the other hand, the first term  $Z^{*(s)}$  on the left-hand side of Eq. (23), which is generated from the dual principal Boltzmann factor after the summation, is not in a gauge invariant form. The duality, however, can transform  $Z^{*(s)}$  into a gauge invariant form. At this time, the form of the edge Boltzmann factor changes from  $\{\exp(\beta J_{ij}) + \exp(-\beta J_{ij}) S_i S_j\} / \sqrt{2}$  to  $\exp(\beta J_{ij} S_i S_j)$  [18],

$$Z^{*(s)} = 2^{N_s^{(s)} - \frac{N_B^{(s)}}{2} - 1} Z_D^{(s)}[x], \quad (36)$$

where  $N_s^{(s)}$  is the number of sites in the cluster of the original square lattice. However the form of the lattice is transformed as shown in Fig. 7. We denote this fact by the subscript D. The application of the duality to the partition function  $Z^{*(s)}$  on the cluster with the dual edge Boltzmann factor enables us to derive a gauge invariant form,

$$Z_D^{(s)}(\beta, \{J_{ij}\}) = \sum_{\{S_i\}} \prod_{(ij)}^{\text{part(D)}} e^{\beta J_{ij} S_i S_j}, \quad (37)$$

where the ‘part(D)’ expresses the product over the bonds on the dual cluster as in Fig. 7. The configurational-averaged quantity of its logarithm can be regarded as the free energy of the random-bond Ising model defined on the dual lattice for the small lattice. We use the relation (36) and rewrite the first term  $Z^{*(s)}$  on the left-hand side

of Eq. (23) as,

$$\begin{aligned} & \left[ \log Z^{*(s)}(\beta, \{J_{ij}\}) \right]_{\text{av}} \\ &= \left[ \log Z_D^{(s)}(\beta, \{J_{ij}\}) \right]_{\text{av}} + \left( N_s^{(s)} - \frac{N_B^{(s)}}{2} - 1 \right) \log 2. \end{aligned} \quad (38)$$

The first term on the right-hand side of this relation can be reduced to the same expression as Eq. (35),

$$\begin{aligned} & \left[ \log Z_D^{(s)}(\beta, \{J_{ij}\}) \right]_{\text{av}} \\ &= \frac{1}{2^{N_D^{(s)}} (2 \cosh \beta_p J)^{N_B^{(s)}}} \\ & \times \sum_{\{J_{ij}\}} Z_D^{(s)}(\beta_p, \{J_{ij}\}) \log Z_D^{(s)}(\beta, \{J_{ij}\}). \end{aligned} \quad (39)$$

Here  $N_D^{(s)}$  expresses the number of sites of the dual cluster, which is equal to that of the plaquettes of the original cluster. In the case of the cluster of the square lattice as in Fig. 7,  $N_s^{(s)} = 1$ ,  $N_B^{(s)} = 4$ ,  $N_D^{(s)} = 4$ . The above considerations enable us to rewrite Eq. (23) as,

$$\begin{aligned} & \frac{1}{2^{N_D^{(s)}}} S_D^{(s)}(\beta_p, \beta) - \frac{1}{2^{N_s^{(s)}}} S^{(s)}(\beta_p, \beta) \\ &= \left( \frac{N_B^{(s)}}{2} - N_s^{(s)} + 1 \right) \log 2, \end{aligned} \quad (40)$$

where

$$\begin{aligned} S_D^{(s)}(\beta_p, \beta) &= \sum_{\{J_{ij}\}} \frac{Z_D^{(s)}(\beta_p, \{J_{ij}\})}{(2 \cosh \beta_p J)^{N_B^{(s)}}} \log \frac{Z_D^{(s)}(\beta, \{J_{ij}\})}{(2 \cosh \beta J)^{N_B^{(s)}}}, \\ S^{(s)}(\beta_p, \beta) &= \sum_{\{J_{ij}\}} \frac{Z^{(s)}(\beta_p, \{J_{ij}\})}{(2 \cosh \beta_p J)^{N_B^{(s)}}} \log \frac{Z^{(s)}(\beta, \{J_{ij}\})}{(2 \cosh \beta J)^{N_B^{(s)}}}. \end{aligned} \quad (41)$$

If we set  $\beta = \beta_p$  in this expression, we find that Eq. (40) states that the multicritical point is located where the difference between two entropies of the distribution of frustration on two lattices related by the duality takes a special value. We can use this expression of the improved technique to lead the structure of the phase diagram such that the gauge symmetry and several correlation inequalities used to give the prediction as in Fig. 1 [4, 5]. It is straightforward to establish the expression as in Eq. (40) also for the case of the triangular lattice.

In the next section, we show the results for the precise locations of the multicritical points obtained by computing Eq. (23) for the square lattice and Eq. (30) for the triangular lattice.



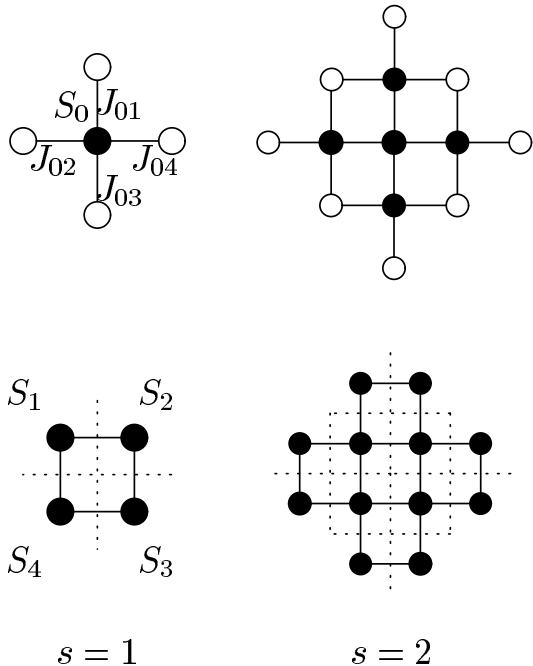


FIG. 8: Two patterns of the clusters for the improved technique on the square lattice. The top figures express the clusters for the evaluations of  $Z^{(s)}$  and  $Z^{*(s)}$ . The bottom figures represent the dual lattices for the clusters, on which the partition functions are denoted by  $Z_D^{(s)}$ . The filled circles are the targets of the summation and white ones are fixed to up directions  $\{S_i\} = 1$ .

## V. DERIVATIONS OF MULTICRITICAL POINTS

We derive the location of the multicritical point by the improved technique for the regular lattices. If we consider a larger range of the summation of spins, (i. e., the cluster includes more bonds and sites.) it is expected that the precision of the improved technique becomes higher. One of the reasons is that the improved technique can include more effects of spatially non-uniform interactions, which are essential features in random spin systems. In other words, the conventional conjecture has been the zeroth approximation without consideration of a form of the lattice and non-uniform interactions in space. The improved technique is also an approximation but gives more precise answers than the conventional conjecture, because it is formulated with the consideration of an individual characteristic of the lattice similarly to the case of the hierarchical lattices. We express the type of the approximations by the value of  $s$ , which has represented the form of the cluster. In this paper, we show the derivations of the multicritical point by use of several types of the clusters for the cases on the square lattice as in Fig. 8 and on the triangular lattice as in Fig. 9.

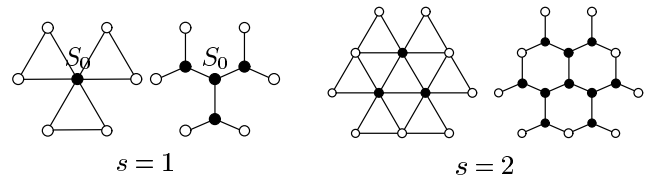


FIG. 9: Two patterns of the clusters for the improved technique on the triangular lattice. The left-hand side for each type of the approximations is for the partition function  $Z_{\text{TR}}^{(s)}$ , and the right-hand side is for the dual partition function  $Z_{\text{TR}}^{*(s)}$ , for which the star-triangle transformation is needed. We use the same symbols as in Fig. 8.

### A. First Approximation for the Square Lattice

We consider the first approximation for the location of the multicritical point on the square lattice by the  $s = 1$  cluster as shown in Fig. 8. To identify the multicritical point, we solve Eq. (23). We first calculate the partition function on the cluster in Eq. (24). The summation over the single spin  $S_0$  at the center surrounded by four bonds ( $J_{01}, J_{02}, J_{03}, J_{04}$ ) with four spins up yields

$$\begin{aligned} Z^{(1)}(\beta, \{J_{ij}\}) &= \sum_{S_0=\pm 1} e^{\beta(J_{01}+J_{02}+J_{03}+J_{04})S_0} \\ &= 2 \cosh\{\beta(J_{01} + J_{02} + J_{03} + J_{04})\}. \end{aligned} \quad (43)$$

Another partition function in Eq. (24) is calculated as,

$$\begin{aligned} Z^{*(1)}(\beta, \{J_{ij}\}) &= \left(\frac{1}{\sqrt{2}}\right)^4 \sum_{S_0=\pm 1} \prod_{i=1}^4 (e^{\beta J_{0i}} + S_0 e^{-\beta J_{0i}}) \\ &= \left(\frac{1}{\sqrt{2}}\right)^4 \left\{ \prod_{i=1}^4 (2 \cosh \beta J_{0i}) + \prod_{i=1}^4 (2 \sinh \beta J_{0i}) \right\}. \end{aligned} \quad (44)$$

This quantity is also obtained from the evaluation of the partition function  $Z_D^{(1)}$  defined on the dual cluster by use of the relation (36). We can explicitly write down the equation for the precise location of the multicritical point for the  $\pm J$  Ising model on the square lattice as, from Eq. (23),

$$\begin{aligned} \sum_{\tau_{ij}} \frac{1}{2^4} \left( 1 + \tanh^4 K_p \prod_{i=1}^4 \tau_{0i} \right) \log \left( 1 + \tanh^4 K \prod_{i=1}^4 \tau_{0i} \right) \\ - \sum_{\tau_{ij}} \frac{1}{2} \frac{2 \cosh \left\{ K_p \sum_{i=0}^4 \tau_{0i} \right\}}{(2 \cosh K_p)^4} \log \frac{2 \cosh \left\{ K \sum_{i=0}^4 \tau_{0i} \right\}}{(2 \cosh K)^4} \\ = 2 \log 2, \end{aligned} \quad (45)$$

where we use the coupling constant  $K = \beta J$  and its sign  $\tau_{ij}$ . Setting  $K = K_p$ , we solve this equation and obtain  $p_c^{(1)} = 0.890725$ . This result is listed in Table II to see the performance of the improvement and to compare the results by the improved technique with the existing ones. Another type of the approximations for the square lattice is by the cluster labeled by  $s = 2$  in Fig. 8 and

$$\int_{-\infty}^{\infty} \prod_{i=1}^4 P(J_{0i}) dJ_{0i} \log \left\{ \prod_{i=1}^4 (2 \cosh \beta J_{0i}) + \prod_{i=1}^4 (2 \sinh \beta J_{0i}) \right\} - \int_{-\infty}^{\infty} \prod_{i=1}^4 P(J_{0i}) dJ_{0i} \log \{ 2 \cosh \{ \beta (J_{01} + J_{02} + J_{03} + J_{04}) \} \} = 2 \log 2, \quad (46)$$

where  $P(J_{ij})$  is the Gaussian distribution function with the mean  $J_0$  and the variance  $J = 1$ . The numerical manipulation of this equation gives the location of the multicritical point for the Gaussian Ising model on the square lattice as  $J_0^{(1)} = 1.021564$ .

### B. Other Approximations for the Square Lattice

We restrict ourselves to the case of the square lattice and consider other types of the improvement. The key of the improvement is the cluster reflecting the shape of the square lattice. We consider here another type of approximations by dividing the square lattice into two clusters, which can cover the whole of the lattice, as in Fig. 10. Then we can reduce the duality relation (11) to,

$$Z_n^{(s,t)}(x_0^{(s)}, x_1^{(s)}, \dots; x_0^{(t)}, x_1^{(t)}, \dots) = Z_n^{(s,t)}(x_0^{*(s)}, x_1^{*(s)}, \dots; x_0^{*(t)}, x_1^{*(t)}, \dots), \quad (47)$$

where  $Z_n^{(s,t)}$  is the reduced partition function after the summation over internal sites on two clusters, and  $x^{(s)}$  and  $x^{(t)}$  are the edge Boltzmann factor including many-body interactions after the summation denoted by  $s$  and  $t$ , respectively. The reduced partition function is regarded as a multi-variable function of two types of arguments  $x^{(s)}$  and  $x^{(t)}$ . We extract the principal Boltzmann factors and assume that a single equation gives the location of the multicritical points,

$$x_0^{(s)} x_0^{(t)} = x_0^{*(s)} x_0^{*(t)}. \quad (48)$$

From this equation, we estimate the location of the multicritical point. For  $s = 1$  and  $t = 1$  small lattices, we obtain  $p_c^{(1,1)} = 0.890794$  and, for  $s = 1$  and  $t = 2$  small lattices,  $p_c^{(1,2)} = 0.890813$ . If the cluster includes many

can be straightforwardly evaluated. The numerical manipulation of this approximation give another prediction  $p_c^{(2)} = 0.890822$  as listed in Table II.

For the Gaussian Ising model, we have to evaluate the quadruple integration over four bonds  $\{J_{ij}\}$  for the improved technique as,

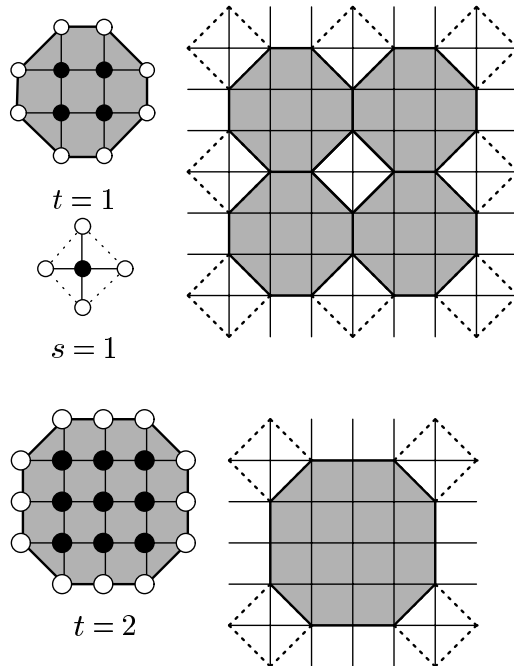


FIG. 10: Other approximations by use of two clusters on the square lattice. The small lattice  $t = 1$  includes 12 bonds and  $t = 2$  has 24 bonds.

bonds, we expect that the improved technique can approach the answer. It is then considered that the multicritical point is located at  $p_c = 0.890813$ . At least, we find that both of the estimations indicate a higher value  $p_c \approx 0.8908$  than  $p_c^{(0)} \approx 0.8900$ , and the precise location of the multicritical point would be  $p_c \approx 0.8908$ .

### C. First Approximation for the Potts Spin Glass

As another application of the improved technique, let us consider the Potts spin glass on the square lattice defined by the Hamiltonian,

$$H = -J \sum_{\langle ij \rangle} \delta(\phi_{ij} + l_{ij}), \quad (49)$$

where  $\phi_{ij} \equiv \phi_i - \phi_j$  expresses the difference between adjacent Potts spins taking an integer value between 0 and  $q - 1$ . The quantity  $l_{ij}$  is the random variable following the distribution function given as

$$P(l_{ij}) = \left\{ \begin{array}{ll} 1 - (q-1)p & (l_{ij} = 0) \\ p & (l_{ij} \neq 0) \end{array} \right\} = \frac{e^{K_p \delta(l_{ij})}}{e^{K_p} + q - 1}, \quad (50)$$

where  $e^{K_p} \equiv \{1 - (q-1)p\}/p$ . This Potts spin glass also has the gauge symmetry. For the Potts spin variables and random variables, we define the gauge transformation as,

$$\phi_i \rightarrow \phi_i + s_i, \quad (51)$$

$$l_{ij} \rightarrow l_{ij} - (s_i - s_j). \quad (52)$$

Here  $s_i$  takes an integer between 0 and  $q - 1$ . Therefore we can establish the Nishimori line by setting  $\beta J = K_p$ , where the internal energy can be calculated exactly and the specific heat can be bounded [27]. The edge Boltzmann factor for the Potts spin glass is given as,

$$x(\phi_{ij}) = e^{\beta J \delta(\phi_{ij} + l_{ij})}, \quad (53)$$

and the dual one is,

$$x^*(\phi_{ij}) = \frac{v}{\sqrt{q}} \left\{ e^{i \frac{2\pi}{q} l_{ij} \phi_{ij}} + \frac{q}{v} \delta(\phi_{ij}) \right\}, \quad (54)$$

where  $v \equiv e^{\beta J} - 1$ .

We thus give the conventional conjecture as follows, [7, 8],

$$\begin{aligned} & -\{1 - (q-1)p\} \log \{1 - (q-1)p\} - (q-1)p \log p \\ & = \frac{1}{2} \log q. \end{aligned} \quad (55)$$

The solutions are obtained as  $p_c = 0.079731$  for  $q = 3$ ,  $p_c = 0.063097$  for  $q = 4$ , and  $p_c = 0.052467$  for  $q = 5$ .

We here estimate the location of the multicritical point for the Potts spin glass on the square lattice by use of the  $s = 1$  small lattice. The partition functions on the cluster as in Eq. (23) are given as,

$$\begin{aligned} Z^{(1)}(\beta; \{l_{ij}\}) &= \left[ \sum_{\{\phi_i\}}^{\text{part}} \prod_{\langle ij \rangle} e^{\beta J \delta(\phi_{ij} + l_{ij})} \right]_{\text{av}}, \end{aligned} \quad (56)$$

$$\begin{aligned} Z^{*(1)}(\beta; \{l_{ij}\}) &= \left[ \sum_{\{\phi_i\}}^{\text{part}} \prod_{\langle ij \rangle} \frac{v}{\sqrt{q}} \left\{ e^{i \frac{2\pi}{q} l_{ij} \phi_{ij}} + \frac{q}{v} \delta(\phi_{ij}) \right\} \right]_{\text{av}}. \end{aligned} \quad (57)$$

We can carry out the summation over  $\phi_0$  at the center of the  $s = 1$  cluster as in Fig. 8 as,

$$\begin{aligned} Z^{(1)}(\beta, \{l_{ij}\}) &= \sum_{\phi_0=0}^{q-1} e^{\beta J \{\delta(\phi_0 + l_{01}) + \delta(\phi_0 + l_{02}) + \delta(\phi_0 + l_{03}) + \delta(\phi_0 + l_{04})\}} \\ &= q + 4v + v^2 \sum_{i \neq j} \delta(l_{0i}, l_{0j}) \\ &\quad + v^3 \sum_{i \neq j \neq k} \delta(l_{0i}, l_{0j}, l_{0k}) + v^4 \delta(l_{01}, l_{02}, l_{03}, l_{04}), \end{aligned} \quad (58)$$

where  $i \neq j$  means the summation over different pairs among four bonds, and  $i \neq j \neq k$  expresses the summation over all combinations of different three bonds among four bonds. In addition, the dual principal Boltzmann factor is given as,

$$\begin{aligned} Z^{*(1)}(\beta, \{l_{ij}\}) &= \left( \frac{v}{\sqrt{q}} \right)^4 \sum_{\phi_0=0}^{q-1} \prod_{i=1}^4 \left\{ e^{i \frac{2\pi}{q} l_{0i} \phi_0} + \frac{q}{v} \delta(\phi_0) \right\} \\ &= \frac{v^4}{q^2} \left\{ \left( 1 + \frac{q}{v} \right)^4 - 1 + q \delta \left( \sum_{i=1}^4 l_{0i} \right) \right\}. \end{aligned} \quad (59)$$

From these quantities, we rewrite Eq. (23) as follows,

$$\left[ \log \left\{ \frac{(q+v)^4 - v^4 + qv^4 \delta \left( \sum_{i=1}^4 l_{0i} \right)}{q + 4v + v^2 \sum_{i \neq j} \delta(l_{0i}, l_{0j}) + v^3 \sum_{i \neq j \neq k} \delta(l_{0i}, l_{0j}, l_{0k}) + v^4 \delta(l_{01}, l_{02}, l_{03}, l_{04})} \right\} \right]_{\text{av}} = 2 \log q, \quad (60)$$

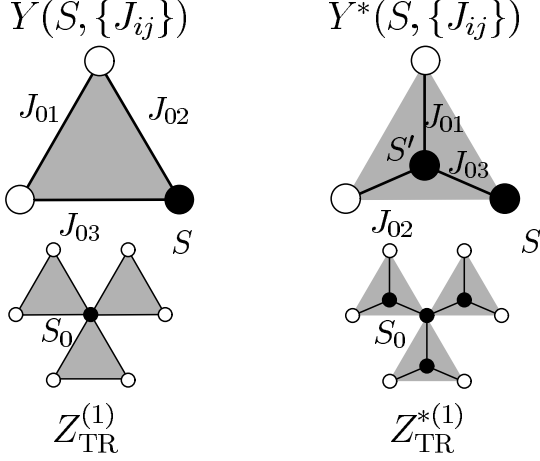


FIG. 11: Relationships between  $Y$  and  $Z_{\text{TR}}^{(1)}$ , and between  $Y^*$  and  $Z_{\text{TR}}^{*(1)}$ . The spin  $S'$  at the center of the star shape is of the summation for the star-triangle transformation.

where the configurational average for the random variables  $\{l_{0i}\}$  on the four bonds follows the distribution function (50). We obtain  $p_c^{(1)} = 0.0791462$  for  $q = 3$ ,  $p_c^{(1)} = 0.0626157$  for  $q = 4$ , and  $p_c^{(1)} = 0.0520578$  for  $q = 5$ . These results are shown in Table II for comparison with those by the conventional conjecture and the existing result by a numerical estimation [28].

#### D. First Approximation for the Triangular Lattice

We show the explicit calculation of the first approximation by the improved technique for the  $\pm J$  Ising model on the triangular lattice. We consider the cluster labeled by  $s = 1$  with three up-pointing triangles as in Fig. 9. In this case, it is convenient to define the following quantities,

$$Y(S, \{J_{ij}\}) = e^{\beta(J_{01} + J_{02}S + J_{03}S)}, \quad (61)$$

$$\begin{aligned} Y^*(S, \{J_{ij}\}) &= \frac{1}{4} \sum_{S'=\pm 1} \prod_{i=1}^2 (e^{\beta J_{0i}} + S' e^{-\beta J_{0i}}) (e^{\beta J_{03}} + S' S e^{-\beta J_{03}}) \\ &= \frac{1}{4} \left\{ \prod_{i=1}^2 (2 \cosh \beta J_{0i}) (e^{\beta J_{03}} + S e^{-\beta J_{03}}) \right. \\ &\quad \left. + \prod_{i=1}^2 (2 \sinh \beta J_{0i}) (e^{\beta J_{03}} - S e^{-\beta J_{03}}) \right\}, \quad (62) \end{aligned}$$

where the locations of the spins  $S'$ ,  $S$ , and the sets of  $\{J_{0i}\}$  are described in Fig. 11. The summation over  $S'$  corresponds to the star-triangle transformation. We

calculate two partition functions for the cluster as, by use of two quantities  $Y$  and  $Y^*$ ,

$$\begin{aligned} Z_{\text{TR}}^{(1)}(\beta, \{J_{ij}\}) &= \sum_{S_0=\pm 1} \prod_{k=1}^3 Y(S_0, \{J_{k,ij}\}) \\ &= 2e^{\beta \sum_{k=1}^3 J_{k,01}} \cosh\left\{\beta \sum_{k=1}^3 (J_{k,02} + J_{k,03})\right\}, \quad (63) \end{aligned}$$

$$\begin{aligned} Z_{\text{TR}}^{*(1)}(\beta, \{J_{ij}\}) &= \sum_{S_0=\pm 1} \prod_{k=1}^3 Y^*(S_0, \{J_{k,ij}\}) \\ &= 2^3 \left\{ \prod_{k=1}^3 \left( \prod_{i=1}^3 \cosh \beta J_{k,0i} + \prod_{i=1}^3 \sinh \beta J_{k,0i} \right) \right. \\ &\quad \left. + \prod_{k=1}^3 \left( \prod_{i=1}^2 \cosh \beta J_{k,0i} \sinh \beta J_{k,03} \right. \right. \\ &\quad \left. \left. + \prod_{i=1}^2 \sinh \beta J_{k,0i} \cosh \beta J_{k,03} \right) \right\}. \quad (64) \end{aligned}$$

Substituting these quantities into Eq. (30), we can obtain the first approximation by the improved technique on the triangular lattice. The result is given as  $p_c^{(1)} = 0.835957$ , which is also listed in Table II with the one  $p_c^{(2)} = 0.835985$  by another approximation by the numerical manipulation of the  $s = 2$  cluster in Fig. 9. Each estimation gives the precise locations of the multicritical point on the hexagonal lattice  $p_c^{(1)} = 0.932611$  and  $p_c^{(2)} = 0.932593$ , by the relation for the mutually dual pair [10],

$$H(p_{\text{TR}}) + H(p_{\text{HEX}}) = 1, \quad (65)$$

where  $H(p)$  is the binary entropy defined by

$$H(p) = -p \log_2 p - (1-p) \log_2 (1-p). \quad (66)$$

Even on the triangular lattice, we can consider the Potts spin glass [29], and apply the improved technique. In this case, we can describe, by the improved technique, a more precise line consisting of the multicritical points on a two-dimensional plane of couplings representing two-body interactions and three-body interactions.

## VI. PERFORMANCE OF IMPROVEMENT

### A. Multicritical Point

We here discuss the performance of the improved technique.

At first, we remark the predictions for the location of the multicritical point of the  $\pm J$  Ising model on the

Type	Conjecture	Numerical result
SQ $\pm J$	$p_c^{(0)} = 0.889972$ [7, 8]	0.8905(5) [19]
	$p_c^{(1)} = 0.890725$	0.8906(2) [20, 21]
	$p_c^{(1,1)} = 0.890794$	0.8907(2) [22]
	$p_c^{(2)} = 0.890822$	0.8894(9) [23]
	$p_c^{(1,2)} = 0.890813$	0.8900(5) [24]
		0.89081(7) [25]
SQ Gaussian	$J_0^{(0)} = 1.021770$ [7, 8]	1.02098(4) [21]
	$J_0^{(1)} = 1.021564$	
TR $\pm J$	$p_c^{(0)} = 0.835806$ [11]	0.8355(5) [24]
	$p_c^{(1)} = 0.835956$	
	$p_c^{(2)} = 0.835985$	
HEX $\pm J$	$p_c^{(0)} = 0.932704$ [11]	0.9325(5) [24]
	$p_c^{(1)} = 0.932611$	
	$p_c^{(2)} = 0.932593$	
SQ Potts( $q = 3$ )	$p_c^{(0)} = 0.079731$ [7, 8]	0.079-0.080 [28]
	$p_c^{(1)} = 0.079146$	
SQ Potts( $q = 4$ )	$p_c^{(0)} = 0.063097$ [8]	–
	$p_c^{(1)} = 0.062616$	
SQ Potts( $q = 5$ )	$p_c^{(0)} = 0.052467$ [8]	–
	$p_c^{(1)} = 0.052058$	

TABLE II: Several predictions for the location of the multicritical point by the improved technique. SQ denotes the square lattice, TR expresses the triangular lattice, and HEX means the hexagonal lattice.

square lattice. All of the results by the improved technique for the  $\pm J$  Ising model on the square lattice indicate a higher value about  $p_c \approx 0.8908$  than  $p_c^{(0)} \approx 0.8900$  by the conventional conjecture. As the size of the cluster increases, the prediction of  $p_c$  converges to some value about  $p_c \approx 0.8908$ . We need the precision to the fourth digit to conclude the conflict between  $p_c \approx 0.8900$ [23, 24] and  $p_c \approx 0.8908$ [19, 20, 21, 22, 25]. For this purpose, the improved technique gives a satisfactory answer that the multicritical point is located at  $p_c \approx 0.8908$ . We cannot completely deny the possibility that the multicritical point locates at  $p_c \approx 0.8900$  as estimated in other studies [23, 24], because the improved technique does not give the exact solution. However the following discussions support our conclusion  $p_c \approx 0.8908$  from a different point of view.

## B. Phase Diagram

The phase boundary can be predicted by the improved technique without the restriction of the Nishimori-line condition, similarly to the conventional conjecture. Unfortunately the improved technique fails again to derive the precise phase boundary especially under the Nishimori line similarly to the case of the hierarchical lattice [14] as in Fig. 12. Nevertheless we find an improve-

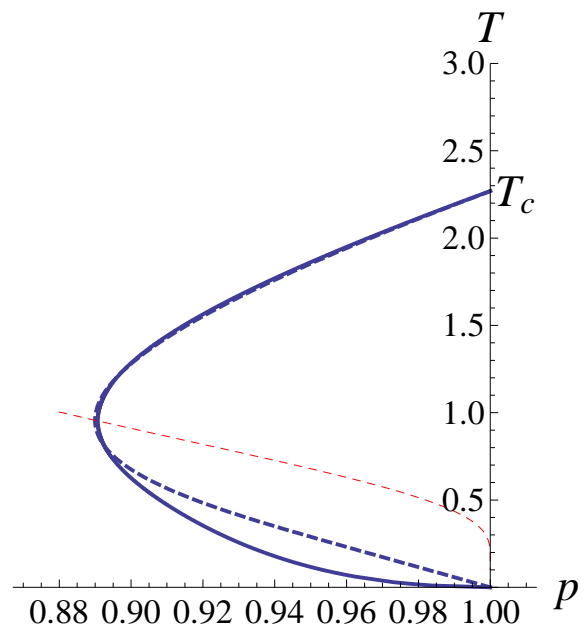


FIG. 12: (Color online) Phase diagram of the  $\pm J$  Ising model on the square lattice by the  $s = 1$  improved technique. The vertical axis is the temperature, and the horizontal axis is the probability for  $J_{ij} = J > 0$  of the  $\pm J$  Ising model. The thick dashed line (blue) is by the conventional conjecture and the thick solid line (blue) is by the improved technique. The thin dashed line (red) is the Nishimori line.

ment of estimations of the slope of the phase boundary at the critical point  $T_c$  of the non-random Ising model. We concentrate on the estimations of the slope and show the results below by use of not only ( $s = 1$ ), ( $s = 2$ ), ( $s = 1, t = 1$ ), and ( $s = 1, t = 2$ ) clusters but also several ones as in Fig. 13. The computing time of the order  $O(2^{N_B^{(s)}})$  is needed in general for the configurational average over  $\{J_{ij}\}$  in evaluation of the improved technique. However, the configurational average becomes much simpler, when we consider a calculation only around  $T_c$  to estimate the slope at  $T_c$ , at which at most a single bond becomes antiferromagnetic. Therefore we can deal with further approximations only to estimate the value of the slope at  $T_c$  by various clusters. The obtained values are listed in Table III. Two types of the approximations, by use of one clusters and by dividing the square lattice into two clusters, give different values but, in any cases, the increase of the size of the cluster shows convergence to the exact solution 3.20911 of the slope at  $T_c$  by Doman [15]. Therefore it is considered that the improved technique gives a systematic way to derive the precise locations of the critical points in the region especially above the Nishimori line.

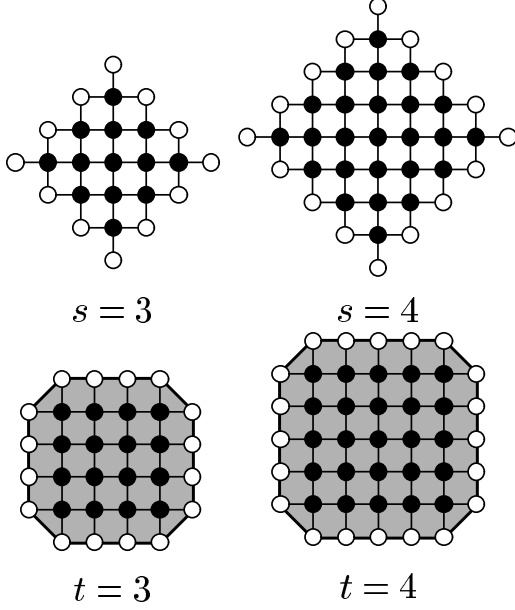


FIG. 13: Several approximations for estimations of the slope at  $T_c$ . The numbers of bonds in each pattern are 36 ( $s = 3$ ), 40 ( $t = 3$ ), 64 ( $s = 4$ ), and 60 ( $t = 4$ ).

### C. Verticality and Reentrance

We also examine the shape of the phase boundary at the multicritical point of the  $\pm J$  Ising model. The following observation also supports the validity of the improved technique. Taking the derivative by  $\beta$  of Eq. (40), we obtain the expression of the slope of the phase boundary at the multicritical point, here denoted by  $\beta_c^{(s)}$ ,

$$\frac{d\beta_p}{d\beta} \Big|_{\beta=\beta_c^{(s)}} = - \frac{\sum_{\{J_{ij}\}} \left( \frac{1}{2^{N_D}} \frac{dZ^*}{d\beta} - \frac{1}{2^{N_s}} \frac{dZ}{d\beta} \right)}{\sum_{\{J_{ij}\}} \left( \frac{1}{2^{N_D}} \frac{dZ^*}{d\beta_p} \log Z^* - \frac{1}{2^{N_s}} \frac{dZ}{d\beta_p} \log Z \right)}, \quad (67)$$

where we omit the approximation type  $s$ , and the arguments of  $Z$  and  $Z^*$  for simplicity. One can find the quantities in the numerator in the right-hand side of this equation being equal to the exact internal energy on the Nishimori line [4, 5],

$$\sum_{\{J_{ij}\}} \frac{1}{2^{N_D}} \frac{dZ^*}{d\beta} = \sum_{\{J_{ij}\}} \frac{1}{2^{N_s}} \frac{dZ}{d\beta} = N_B \tanh \beta_p J. \quad (68)$$

Hence the slope of the phase boundary at the multicritical point should be vertical. In other words, the multicritical point is located at a minimum value  $p_c$  on the phase boundary predicted by the improved technique. This statement is satisfied for any clusters. Therefore,

Type	Number	Value of slope
$s = 0$	1	3.41421
$s = 1$	4	3.33658
$s = 2$	16	3.31272
$s = 3$	32	3.29352
$s = 4$	64	3.28161
exact		3.20911 [15]

Type	Number	Value of slope
$s = 0$	1	3.41421
$s = 1, t = 1$	4 + 12	3.31225
$s = 1, t = 2$	4 + 24	3.29414
$s = 1, t = 3$	4 + 40	3.28170
$s = 1, t = 4$	4 + 60	3.27287
exact		3.20911 [15]

TABLE III: Slope at the critical point  $T_c$  for the  $\pm J$  Ising model on the square lattice. The top table gives the results by the clusters with many cross shapes denoted by  $s$ . The bottom table shows those by two clusters represented by  $(s, t)$ . For comparison, we write the result by the conventional conjecture denoted by  $s = 0$ .

even if we consider the infinite size of the small lattice in which we can expect to obtain the exact answer, the verticality at the multicritical point holds. The improved technique can give the consistent phase boundary with the predicted by the gauge symmetry [4, 5].

The second derivative yields a non-zero value of  $d^2\beta_p/d\beta^2$ , which is proportional to the difference of the specific heat between  $\pm J$  Ising models on two clusters,

$$\frac{d^2\beta_p}{d\beta^2} \Big|_{\beta=\beta_c^{(s)}} = - \frac{\sum_{\{J_{ij}\}} \left\{ \frac{1}{2^{N_D}} \frac{1}{Z^*} \left( \frac{dZ^*}{d\beta} \right)^2 - \frac{1}{2^{N_s}} \frac{1}{Z} \left( \frac{dZ}{d\beta} \right)^2 \right\}}{\sum_{\{J_{ij}\}} \left( \frac{1}{2^{N_D}} \frac{dZ^*}{d\beta_p} \log Z^* - \frac{1}{2^{N_s}} \frac{dZ}{d\beta_p} \log Z \right)}, \quad (69)$$

We do not have the exact value of the specific heat on the Nishimori line though we know an upper bound [4, 5]. We cannot completely determine the shape of the phase boundary only by the improved technique. However we remark that the estimated values of the second derivative become lower, if the cluster under consideration become larger as 0.956729 ( $s = 0$ ), 0.753892 ( $s = 1$ ), and 0.737262 ( $s = 2$ ). These positive values indicate that the phase boundary predicted by the improved technique become reentrant or vertical. The possibility of the phase boundary is indeed limited into whether vertical or reentrant as rigorously shown by the gauge-symmetry argument [4, 5].

### D. Other Random Spin Systems

If the improvement affects the predictions not only of the multicritical point but also for other critical points, we can apply the improved technique to random spin systems without gauge symmetry. The absence of the Nishimori line on the phase diagram does not permit us to rewrite Eq. (23) as Eq. (40), which can give a relation between two entropies of the distribution of frustration. However the previous discussions by the duality for the cluster are applicable to various random spin models. We then give the critical points by the following equation even for random spin systems without the Nishimori line,

$$-\beta \left( \left[ F_D^{(s)} \right]_{\text{av}} - \left[ F^{(s)} \right]_{\text{av}} \right) = \left( \frac{N_B^{(s)}}{2} - N_s^{(s)} + 1 \right) \log 2, \quad (70)$$

where  $\left[ F^{(s)} \right]_{\text{av}}$  is the free energy on the cluster, and  $\left[ F_D^{(s)} \right]_{\text{av}}$  represents that on the dual cluster. Therefore our task to analytically derive the critical points in random spin systems is to estimate the difference between the two free energies on the cluster and its dual one.

We apply the improved technique to the bond-diluted Ising model by the evaluation of Eq. (70) by use of the distribution function,

$$P(J_{ij}) = p\delta(J_{ij} - J) + (1 - p)\delta(J_{ij}). \quad (71)$$

The predicted phase boundary in Fig. 14 is not drastically different from the one by the conventional conjecture [30]. However we can find a significant difference by investigation of the values of the slope at  $T_c$  similarly to the case of the  $\pm J$  Ising model. We show the results for the slope at  $T_c$  for the bond-diluted Ising model in Table IV. The estimated values for the square lattice shows convergence to the exact solution 1.32926 [16], similarly to the case for the  $\pm J$  Ising model.

In addition, we remark that the improved technique works very well for the critical points of the bond-diluted  $q$ -state Potts model, and  $q$ -state Villain model [31]. From these points of view, we conclude that the improved technique is also a systematic approach leading to the precise locations of the critical points in broader classes of the random spin systems.

## VII. CONCLUSION

We proposed an improved technique applicable to the square, triangular, hexagonal lattices, and derived the precise locations of the multicritical points for the  $\pm J$  Ising model, the Gaussian Ising model, and the Potts spin glass on the square lattice, as well as the  $\pm J$  Ising model on the triangular lattice and the hexagonal lattice. This improved technique is still approximation for the location

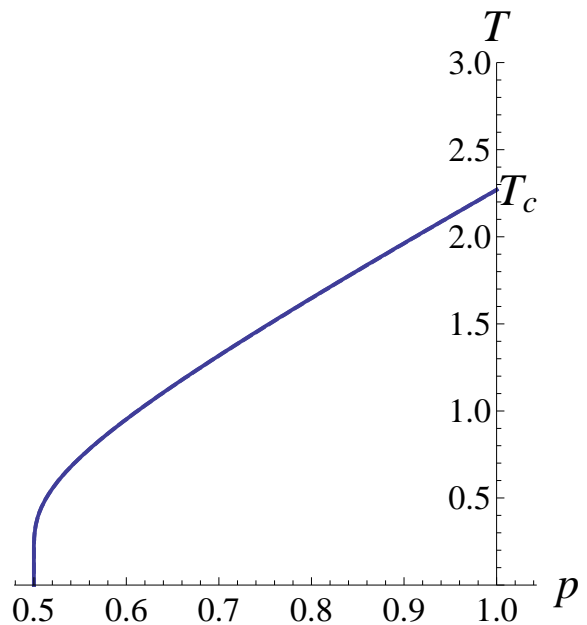


FIG. 14: (Color online) Phase diagram of the bond-diluted Ising model on the square lattice by the  $s = 1$  improved technique. The vertical axis is the temperature, and the horizontal axis is the probability for  $J_{ij} = J > 0$ .

Type	Number	Value of slope
$s = 0$	1	1.34254
$s = 1$	4	1.33780
$s = 2$	16	1.33626
$s = 3$	32	1.33500
$s = 4$	64	1.33420
exact		1.32926 [16]

Type	Number	Value of slope
$s = 0$	1	1.34254
$s = 1, t = 1$	4 + 12	1.33623
$s = 1, t = 2$	4 + 24	1.33504
$s = 1, t = 3$	4 + 40	1.33421
$s = 1, t = 4$	4 + 60	1.33362
exact		1.32926 [16]

TABLE IV: Slope at  $T_c$  for the bond-diluted Ising model on the square lattice. For comparison, we write the result by the conventional conjecture denoted by  $s = 0$ .

of the multicritical point. However we can enhance the precision of the approximation by the summation over spins in the cluster taken from the considered lattice, if we need the precise location of the critical points in a random spin system. This would open a way to analytically derive the location of the critical points in random spin systems with very high precision. Unfortunately, in the low-temperature region under the Nishimori line, the

improved technique cannot give satisfactory answers yet. We solve this problem in the low-temperature region under the Nishimori line, and have to examine the validity of some hypotheses on the improved technique.

In this paper, we restrict ourselves to the random spin systems in two-dimensional systems. However we can apply the duality to other dimensional systems. For example, the duality can transform the random-bond Ising model on the three-dimensional cubic lattice into the random-plaquette gauge model on the three-dimensional cubic lattice. The random-plaquette gauge model is an attractive one in terms of the quantum toric code [32, 33]. An accuracy threshold to correct error of the quantum toric code corresponds to the location of the multicritical point on the random-plaquette gauge model with the random couplings following the  $\pm J$  distribution function on the three-dimensional cubic lattice. The conventional conjecture relates this threshold with the location of the multicritical point of the  $\pm J$  Ising model on the three-dimensional cubic lattice [9]. The improved technique also cannot directly derive such an accuracy threshold, but can make more precise relationship between the locations of the multicritical points on the random-bond Ising model and the random-plaquette gauge model.

As another direction of studies in the future, we should

clarify the physical meaning of the equation consisting of the entropy of the distribution of frustration, which determines the location of the multicritical point.

### Acknowledgments

The author greatly acknowledges the fruitful discussion with Prof. H. Nishimori, Prof. A. N. Berker and Dr. M. Hinczewski, and sincerely thanks Prof. Y. Okabe for sending unpublished numerical data of the bond-diluted Potts model and the bond-diluted Villain model, and Prof. M. Picco, who informed him of a his recent result of the multicritical point on the square lattice. He would like to also thank Prof. S. L. A. de Queiroz for a valuable comment and Dr. K. Takahashi for reading the manuscript and giving stimulating comments. This work was partially supported by the Ministry of Education, Science, Sports and Culture, Grant-in-Aid for Young Scientists (B) No. 20740218, and for scientific Research on the Priority Area “Deepening and Expansion of Statistical Mechanical Informatics (DEX-SMI)”, and by CREST, JST.

- 
- [1] D. Sherrington and S. Kirkpatrick, *Phys. Rev. Lett.* **35**, 1792 (1975).
  - [2] K. Binder and A. P. Young, *Rev. Mod. Phys.* **58**, 801 (1986).
  - [3] M. Mézard, G. Parisi, and M. Virasoro, *Spin Glass Theory and Beyond* (World Scientific, 1986).
  - [4] H. Nishimori, *Prog. Theor. Phys.* **66**, 1169 (1981).
  - [5] H. Nishimori, *Statistical Physics of Spin Glasses and Information Processing: An Introduction* (Oxford Univ. Press, Oxford, 2001).
  - [6] H. Nishimori, *J. Phys. Soc. Jpn.* **55**, 3305 (1986).
  - [7] H. Nishimori and K. Nemoto, *J. Phys. Soc. Jpn.* **71**, 1198 (2002).
  - [8] J.-M. Maillard, K. Nemoto, and H. Nishimori, *J. Phys. A* **36**, 9799 (2003).
  - [9] K. Takeda, and H. Nishimori, *Nucl. Phys. B* **686**, 377 (2004).
  - [10] K. Takeda, T. Sasamoto, and H. Nishimori, *J. Phys. A* **38**, 3751 (2005).
  - [11] H. Nishimori and M. Ohzeki, *J. Phys. Soc. Jpn.* **75**, 034004 (2006).
  - [12] H. Nishimori, *J. Stat. Phys.* **126**, 977 (2007).
  - [13] M. Hinczewski and A. N. Berker, *Phys. Rev. B* **72**, 144402 (2005).
  - [14] M. Ohzeki, H. Nishimori, and A. N. Berker, *Phys. Rev. E* **77**, 061116 (2008).
  - [15] E. Domany, *J. Phys. C* **12**, L119 (1979).
  - [16] E. Domany, *J. Phys. C* **11**, L337 (1978).
  - [17] H. A. Kramers and G. H. Wannier, *Phys. Rev.* **60**, 252 (1941).
  - [18] F. Y. Wu and Y. K. Wang, *J. Math. Phys.* **17**, 439 (1976).
  - [19] F. D. A. Aarão Reis, S. L. A. de Queiroz, and R. R. dos Santos, *Phys. Rev. B* **60**, 6740 (1999).
  - [20] A. Honecker, M. Picco, and P. Pujol, *Phys. Rev. Lett.* **87**, 047201 (2001).
  - [21] M. Picco, A. Honecker, and P. Pujol, *J. Stat. Mech.* P09006 (2006).
  - [22] F. Merz and J. T. Chalker, *Phys. Rev. B* **65**, 054425 (2002).
  - [23] N. Ito and Y. Ozeki, *Physica A* **321**, 262 (2003).
  - [24] S. L. A. de Queiroz, *Phys. Rev. B* **73**, 064410 (2006).
  - [25] M. Hasenbusch, F. P. Toldin, A. Pelissetto, and E. Vicari, *Phys. Rev. E* **77**, 051115 (2008).
  - [26] F. Y. Wu, *Rev. Mod. Phys.* **54**, 235 (1982).
  - [27] H. Nishimori and M. J. Stephen, *Phys. Rev. B* **27**, 5644 (1983).
  - [28] J. L. Jacobsen and M. Picco, *Phys. Rev. E* **65**, 026113 (2002).
  - [29] M. Ohzeki, *J. Phys. Jpn.* **76**, 114003 (2007).
  - [30] H. Nishimori, *J. Phys. C* **12**, L641 (1979).
  - [31] Y. Okabe, private communication.
  - [32] E. Dennis, A. Kitaev, A. Landahl, and J. Preskill, *J. Math. Phys.* **43**, 4452 (2002).
  - [33] C. Wang, J. Harrington, and J. Preskill, *Ann. Phys. (NY)* **303**, 31 (2003).